
This item was submitted to [Loughborough's Research Repository](#) by the author.
Items in Figshare are protected by copyright, with all rights reserved, unless otherwise indicated.

pH-sensitive micelles for targeted drug delivery prepared using a novel membrane contactor method

PLEASE CITE THE PUBLISHED VERSION

<http://dx.doi.org/10.1021/am4018237>

PUBLISHER

© American Chemical Society

VERSION

AM (Accepted Manuscript)

LICENCE

CC BY-NC-ND 4.0

REPOSITORY RECORD

Laouini, Abdallah, Konstantinos P. Koutroumanis, Catherine Charcosset, Stella Georgiadou, Hatem Fessi, R.G. Holdich, and Goran T. Vladisavljevic. 2014. "Ph-sensitive Micelles for Targeted Drug Delivery Prepared Using a Novel Membrane Contactor Method". figshare. <https://hdl.handle.net/2134/14434>.

This item was submitted to Loughborough's Institutional Repository (<https://dspace.lboro.ac.uk/>) by the author and is made available under the following Creative Commons Licence conditions.



For the full text of this licence, please go to:
<http://creativecommons.org/licenses/by-nc-nd/2.5/>

pH-Sensitive micelles for targeted drug delivery

prepared using a novel membrane contactor

method

Abdallah Laouini,^{†,‡} Konstantinos P. Koutroumanis,[‡] Catherine Charcosset,[†] Stella Georgiadou,[‡] Hatem Fessi,[†] Richard G. Holdich,[‡] and Goran T. Vladisavljević^{,†}*

[†]Université Claude Bernard Lyon 1, Laboratoire d'Automatique et de Génie des Procédés (LAGEP), UMR-CNRS 5007, CPE Lyon, Bat 308 G, 43 Boulevard du 11 Novembre 1918, F-69622 Villeurbanne Cedex, France.

[‡]Department of Chemical Engineering, Loughborough University, Loughborough, LE11 3TU, United Kingdom.

*Corresponding author's address: Department of Chemical Engineering, Loughborough University, Loughborough, LE11 3TU, United Kingdom. Phone number +441509222518; fax number +441509223923; email: g.vladisavljevic@lboro.ac.uk

ABSTRACT: A novel membrane contactor method was used to produce size-controlled poly(ethylene glycol)-b-polycaprolactone (PEG-PCL) copolymer micelles composed of diblock copolymers with different average molecular weights, M_n (9200 or 10400 Da) and hydrophilic fractions, f (0.67 or 0.59). By injecting $570 \text{ l m}^{-2} \text{ h}^{-1}$ of the organic phase (a 1 mg

ml⁻¹ solution of PEG-PCL in tetrahydrofuran) through a microengineered nickel membrane with a hexagonal pore array and 200 μm pore spacing into deionized water agitated at 700 rpm, the micelle size linearly increased from 92 nm for a 5-μm pore size to 165 nm for a 40-μm pore size. The micelle size was finely tuned by the agitation rate, transmembrane flux and aqueous to organic phase ratio. An encapsulation efficiency of 89 % and a drug loading of ~75 % (w/w) were achieved when a hydrophobic drug (vitamin E) was entrapped within the micelles, as determined by ultracentrifugation method. The drug-loaded micelles had a mean size of 146 ± 7 nm, a polydispersity index of 0.09 ± 0.01, and a zeta potential of -19.5 ± 0.2 mV. When drug-loaded micelles were stored for 50 h, a pH sensitive drug release was achieved and a maximum amount of vitamin E (23 %) was released at the pH of 1.9. When a pH-sensitive hydrazone bond was incorporated between PEG and PCL blocks, no significant change in micelle size was observed at the same micellization conditions.

KEYWORDS: Polymeric micelles; pH-sensitivity; Membrane contactor; Stirred cell; Vitamin E encapsulation; Hydrazone bond.

INTRODUCTION

In recent years, there has been growing interest in drug delivery using nano-carriers such as liposomes, core-shell nanocapsules, solid lipid nanoparticles, and micelles. Polymeric micelles are self-assembled aggregates of amphiphilic polymers consisting of a hydrophobic inner core and hydrophilic outer shell.¹ The core can be used to solubilize drugs with poor water solubility, while the hydrophilic shell can prolong circulation time in blood by

inhibiting opsonins from adsorption on the micelle surface. Long circulation time in vivo is ensured by the micelle size of less than 200 nm.² Particles with such a small size remain undetected by reticuloendothelial systems (RES),³ which can be exploited to achieve prolonged therapeutic action.⁴

Micelles can be modified by incorporation of various functional groups and bonds to achieve targeted or triggered release. Of the many stimuli that can be exploited, changes in pH are particularly interesting because significant pH gradients can be found physiologically, for instance between normal tissues and some pathological sites, between the extracellular environment and some cellular compartments, and along the gastrointestinal tract. Some pathological states are associated with pH profiles different from that of normal tissues. Examples include ischemia, infection, inflammation and tumor acquisition, which are often associated with acidosis.⁵ Compared to normal blood pH of 7.4, extracellular pH values in cancerous tissues can be as low as 5.7 due to rapid expansion of tumor cells, leading to production of lactic acid and hydrolysis of ATP in an energy-deficient manner.⁶ To achieve pH sensitivity, the hydrophobic block of the copolymer can be modified to introduce acid-labile bonds which degrade at mildly acidic pH, causing the micelle to collapse, thus releasing the encapsulated drug. The examples of pH sensitive groups are acetal bonds⁷⁻⁸ and poly(ortho ester) side chains⁹ that allow chemical conjugation of drugs to the side chain.

There is a plethora of methods available for the preparation of polymeric micelles. If a copolymer is soluble in water, micellization is usually performed by direct dissolution in water or film casting. If a copolymer is insoluble in water, the most common methods are dialysis, oil-in-water (O/W) emulsion and co-solvent evaporation or displacement. The direct dissolution consists of dissolving polymer and drug in water. The method is not widely

applicable, since both blocks of the copolymer and the drug should be readily soluble in water. The method has been applied successfully for the encapsulation of hydrophobic drugs, but produced micelles are large and polydisperse.¹⁰ In film casting, polymer and drug are dissolved in a volatile organic solvent, which after evaporation leaves a thin drug-impregnated film. Micelles are formed upon addition of warm water and stirring. The method is often used when other methods give poor drug loading efficiencies, as is the case with paclitaxel.¹¹ Micelles produced by film casting typically have large sizes and bimodal size distributions.¹² In order to avoid detection by the RES and premature elimination, the micelle solution must be filtered, which results in drug losses and poor yields. In the dialysis method, drug and polymer are dissolved in a water-miscible organic solvent followed by dialysis to replace the organic solvent with water. The technique generally yields large micelles with low drug contents¹³ and lacks reproducibility.¹⁴ These problems can be partially addressed by adding water to the polymer/drug solution prior to the dialysis, which kinetically freezes the micelles.¹⁵ Dialysis often requires days to complete and is difficult to scale up. In the O/W emulsion technique, polymer and drug are dissolved in a water-immiscible organic solvent and this mixture is then emulsified followed by evaporation of the organic solvent. The co-solvent evaporation method is similar, except that the organic solvent is miscible with water.¹⁶ This method is often more suitable than the emulsion method, since it leads to the formation of smaller micelles with higher drug loading¹⁷ and ICH (International Conference on Harmonization) class 2 solvents, such as chloroform and dichloromethane, can be avoided.¹⁸ Therefore, most of the established techniques for micelle formation are not suitable for scaling-up from laboratory level to industrial production and suffer from low

reproducibility and poor control over the micelle size.¹⁹ Thus, there is a strong need for improvements in micelle preparation techniques.

The main objective of this work was to develop and investigate a novel membrane dispersion method for micelle preparation, suitable for large scale production. Membranes are increasingly used for fabrication of emulsions and particles²⁰ including nanoparticles such as solid lipid nanoparticles,²¹ liposomes,²² and nanoemulsions.²³ However, to the best of our knowledge, fabrication of micelles by dispersion through a microporous membrane has never been reported.

EXPERIMENTAL SECTION

Reagents. Poly(ethylene glycol) methyl ether (Mn ~5000 Da) (PEG), ϵ -caprolactone monomer 99% (ϵ -CL), tin(II) 2-ethylhexanoate 95%, Sn(Oct)₂, and sodium silicotungstate were supplied by Sigma-Aldrich. Toluene, extra dry grade, was purchased from Acros Organics. PEG was dried by azeotropic distillation with toluene prior to the polymerization reaction. ϵ -CL was dried prior use by distillation under reduced pressure onto 3A molecular sieves. O-[2-(6-Oxocaproylamino)ethyl]-O'-methylpolyethylene glycol (Mn = 5000 g/mol), PEG-CHO, and 2-hydroxyethylhydrazine 98%, 2-HEH, were purchased from Sigma-Aldrich Co Ltd, Gillingham, Dorset, UK. Tetrahydrofuran (THF) and acetone of analytical grade were purchased from Fischer Scientific and used without further purification. Ultra-pure water was obtained from a Millipore Synergy® system (Ultrapure Water System, Millipore).

Equipment. The micelles suspension was prepared using a stirred cell with a flat disc membrane fitted under the paddle blade stirrer, as shown in Figure 1 (a).

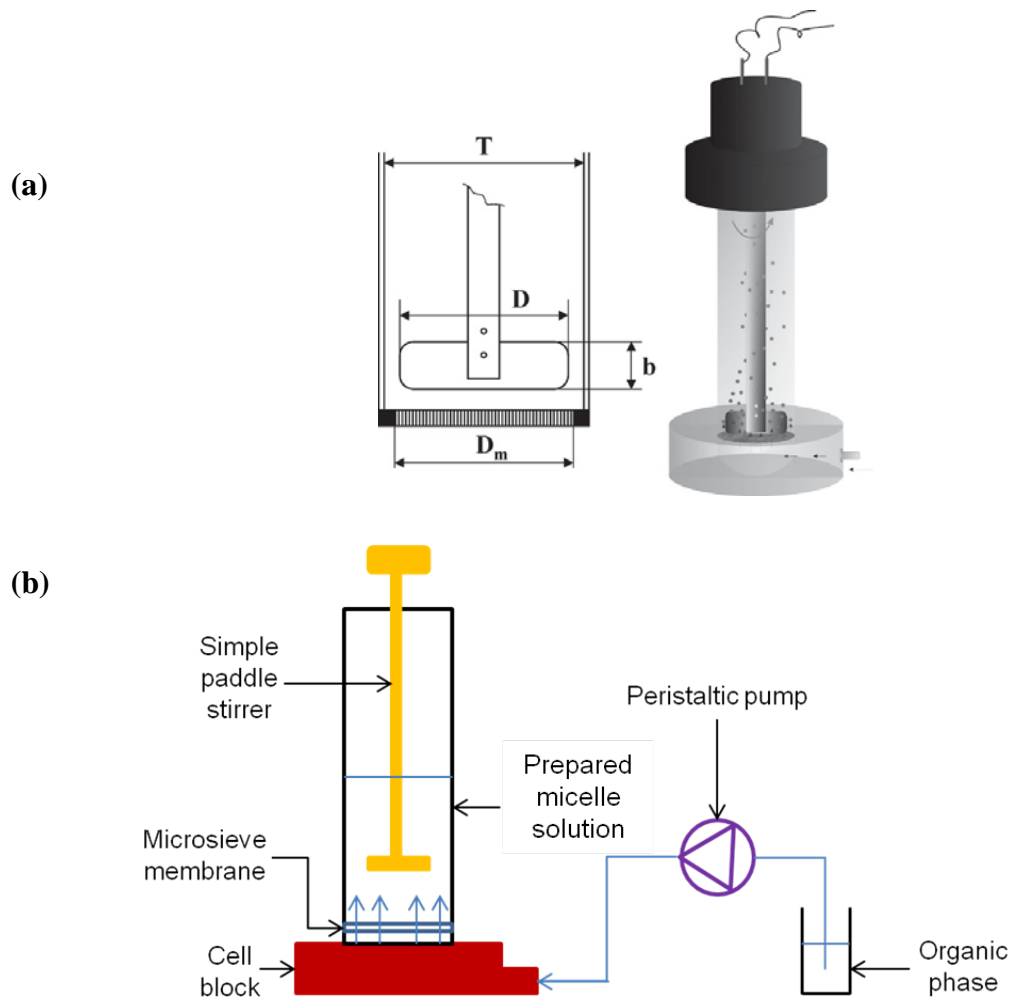


Figure 1. (a) Schematic illustration of the stirred cell with simple paddle stirrer above a flat disc membrane ($b = 12$ mm, $D = 32$ mm, $D_m = 33$ mm, and $T = 40$ mm). (b) Schematic diagram of the experimental set-up.

Both stirred cell and membranes were supplied by Micropore Technologies Ltd. (Hatton, Derbyshire, UK). The agitator was driven by a 24 V DC motor (INSTEK model PR 3060) and the paddle rotation speed was controlled by the applied voltage. The membranes used

were nickel membranes with regular hexagonal pore array containing uniform cylindrical pores with a diameter of 5, 10, 20 or 40 μm , arranged at uniform spacing of 80 or 200 μm (Figure S1 in the supporting information). The membranes were fabricated by the UV-LIGA (ultraviolet lithography, electroplating, and molding) process, which involves galvanic deposition of nickel onto the template formed by photolithography.²⁴

The porosity of a membrane with the hexagonal pore array is given by:

$$\varepsilon = \frac{\pi}{2\sqrt{3}} \left(\frac{d_p}{S} \right)^2 \quad (1)$$

where d_p is the pore diameter and S is the interpore distance. The porosities of the membranes calculated from Eq. (1) are given in the supporting information (Table S1).

Preparation Procedures. *PEG-PCL Synthesis.* 1 g of PEG and 40% (v/v) ε -CL solution in toluene were dissolved in 20 ml of refluxing toluene under nitrogen atmosphere. The mole ratio of PEG to ε -CL in the reaction mixture varied from 1:22 to 1:88. The polymerization was initiated by the addition of a 20% (v/v) solution of $\text{Sn}(\text{Oct})_2$ in toluene (0.75 w/w) and carried out at 110 $^\circ\text{C}$ under nitrogen atmosphere and constant stirring for 18 h. The PEG-PCL copolymer was isolated by precipitation in diethyl ether and dried under vacuum.

PEG-Hyd-PCL Synthesis. 1 g of PEG-CHO was dissolved in 12 ml of ethanol at 35 $^\circ\text{C}$ under nitrogen atmosphere and 2-HEH 10% (v/v) solution in ethanol was added in excess ($\text{CHO}/\text{NHNH}_2 = 1:5$). After 48 h, PEG-Hyd-OH was isolated from diethyl ether, washed with cold (-18 $^\circ\text{C}$) ethanol and dried under vacuum at 40 $^\circ\text{C}$ for 24 h. Polymerization of ε -CL from

PEG-Hyd-OH was carried out under the same conditions used in synthesis of PEG-PCL copolymers.

Micellization and Drug Loading. A schematic diagram of the experimental set-up is shown in Figure 1 (b). The cell was filled with 15-35 ml of ultrapure water and the stirring speed was adjusted between 400 and 1000 rpm. A 1 mg ml⁻¹ of the copolymer (PEG-PCL-3 or PEG-PCL-4) was prepared by dissolving the copolymer in THF or acetone. The organic phase was injected through the membrane using a peristaltic pump (Watson Marlow 101U, Cornwall, UK) at a constant flow rate of 2-8 ml min⁻¹ corresponding to the dispersed phase flux of 142-568 l m⁻² h⁻¹. The experiment was run until a predetermined organic to aqueous phase ratio was achieved. Spontaneous formation of micelles started as soon as the organic phase was brought in contact with the aqueous phase, but the micelle suspension was kept under stirring for 15 min. The suspension was then collected and the organic solvent was removed by stirring under vacuum for 24 h. After each experiment, the membrane was sonicated in THF for 1 h, followed by soaking in a siloxane-based wetting agent for 30 min. Drug-loaded micelles were prepared as described above with the only difference being that 2.5 mg ml⁻¹ vitamin E was dissolved in the organic phase containing the polymer.

Polymers Characterization. *Gel Permeation Chromatography (GPC).* GPC analysis was performed on an Agilent 1100 HPLC System equipped with a refractive index detector (G1362A) and an Agilent PLgel MIXED-C column, 5 µm, 300 × 7.5 mm, in series with an Agilent PLgel guard column, 5 µm, 50 × 7.5 mm. The flow rate of the mobile phase (THF) was 1 ml min⁻¹ and the column temperature was 30 °C. The calibration was performed using polystyrene standards with a narrow molecular weight distribution (EasiVials PS-M).

Fourier Transformed-Infrared Spectroscopy (FTIR). FTIR spectra were obtained using a Shimadzu FTIR-8400S spectrometer. A small amount of each material was mixed with KBr and compressed to tablets. The IR spectra of these tablets were obtained in absorbance mode and in the spectral region of 600 to 4000 cm^{-1} using a resolution of 4 cm^{-1} and 64 co-added scans.

Nuclear Magnetic Resonance Spectroscopy (NMR). Polymers were solubilised in deuterated chloroform (CDCl_3) and ^1H -NMR spectra were obtained on a Bruker Ultrashield Av-400 spectrometer, operating at 400.13 MHz, employing a 5 mm high-resolution broad-band ATMA gradients probe. Spectra were recorded using the zg30 pulse program with $P_{90} = 14.5 \mu\text{s}$ covering a sweep width of 20.7 ppm (8278 Hz) with 64 k time domain data points giving an acquisition time of 3.95 s, Fourier transformed using 128 k data points and referenced to an internal TMS standard at 0.0 ppm.

Micelles Characterization. *Particle Size Analysis.* Particle size distribution was determined by dynamic light scattering (DLS), otherwise known as photon correlation spectroscopy (PCS),²⁵⁻²⁶ using a Malvern Zetasizer Nano-series (Malvern Instruments Zen 3600, Malvern, UK). Each sample was diluted 10-fold with ultra-pure water before measurement and analyzed in triplicate at 25 °C. The particle size distribution data were generated using the DTS nano software (version 5.2). The micelle size polydispersity was expressed by the polydispersity index, PDI.

Zeta Potential. The zeta potential was determined using a Malvern Zetasizer Nano-series (Malvern Instruments Zen 3,600, Malvern UK) and measurements were performed at least

three times after dilution in water. The zeta potential was calculated from the electrophoretic mobility applying the Helmholtz-Smoluchowski equation.²⁷

Encapsulation Efficiency. The encapsulation efficiency of vitamin E in micelles was determined using the ultracentrifugation technique. The total amount of vitamin E (TA) was determined after disrupting drug-loaded micelles in ethanol using an ultrasound bath for 10 min. The amount of vitamin E encapsulated in micelles (EA) was determined by centrifuging solutions of vitamin E-loaded micelles using an Optima™ Ultracentrifuge (Beckman Coulter, USA) at 50,000 rpm for 50 min at +4 °C to separate micelles from non-encapsulated drug. The resulting micelle sediment was dissolved in ethanol and assayed for encapsulated vitamin E content (EA). The vitamin E encapsulation efficiency (E.E.) was calculated as follows:

$$E.E. = EA/TA \times 100 \quad (2)$$

E.E. was determined in triplicate. The concentration of vitamin E was measured using an HPLC system (Agilent System series 1100, Agilent Technologies, California, USA) consisted of a pump, an auto-sampler and a UV/VIS detector. The column used was a LiChrospher RP C18 column (5 µm, 15 cm × 0.46 cm) (Supelco, Bellefonte, USA). The separation was carried out using a mixture of methanol and water (96:4 v/v) as the mobile phase at a flow rate of 1.6 ml min⁻¹. The eluent was monitored at 292 nm and peaks were recorded using the chromatography data system software provided by Agilent. The column was equilibrated for 30 min with a minimum of 30 column volumes. The column was washed after use using water - acetonitrile mixture (50:50 v/v) for 60 min. This HPLC analytical method was validated (data not shown).

Transmission Electron Microscopy (TEM). TEM observation was carried out according to a previously reported protocol.²⁸ Briefly, an aliquot of the micelle solution was diluted 10-fold using ultrapure water and a drop of the diluted sample was placed onto a carbon-coated copper grid. The sample was allowed to stand for 3 min, after which the excess fluid was absorbed by a filter paper leaving a thin liquid film over the holes. One drop of a 1% (w/w) sodium silicotungstate solution was then applied and allowed to dry for 2 min. Finally, the stained samples were observed and images were taken using a CM 120 microscope (Philips, Eindhoven, Netherlands) operating at an accelerating voltage of 80 kV.

Process Reproducibility. The experiments conducted under the optimum conditions were repeated three times in order to estimate reproducibility of the fabrication process.

pH-Responsive Drug Release. A drug-loaded micelle solution was divided into 4 aliquots and the pH of each aliquot was adjusted to 1.9, 4.5, 6.3 and 9.8. pH 1.9 was adjusted by potassium phosphate buffer consisting of potassium dihydrogen phosphate and phosphoric acid solution. pH 4.5 or 6.3 was adjusted by a buffer solution of potassium dihydrogen phosphate and sodium hydrogen phosphate. At pH 9.8, the drug release medium was a buffer solution of boric acid and potassium borate. At chosen time intervals, samples were taken and encapsulation efficiency was determined using the method previously described.

RESULTS AND DISCUSSION

Polymer Characterization. *Gel Permeation Chromatography (GPC)*. The molecular weight of the synthesized polymers, as calculated by GPC, is shown in Table 1. The hydrophilic fraction, f , is the mass fraction of the hydrophilic block to the total polymer mass and it dictates the structure of the micelles. For diblock amphiphilic copolymers, Discher and

Eisenberg²⁹ suggest that micelles are formed if $f > 0.5$; a condition that is satisfied for all four synthesized polymers.

Table 1. Number average molecular weight, M_n , polydispersity index, M_w/M_n , and hydrophilic fraction, f , of the synthesized copolymers, as determined by GPC.

Polymer	PEG/ ϵ -CL mole ratio in the feed mixture	M_n (Da)	M_w/M_n	f
PEG-PCL-1	1:22	7400	1.10	0.82
PEG-PCL-2	1:44	8200	1.14	0.74
PEG-PCL-3	1:66	9200	1.17	0.67
PEG-PCL-4	1:88	10400	1.25	0.59

Fourier Transformed-Infrared Spectroscopy (FTIR). FT-IR spectra are presented in Figure 2. All materials show characteristic absorbancies for PEG, the C-O-C etheric bond bending vibration at 1109 cm^{-1} and the absorbancies at 842 and 1333 cm^{-1} , attributed to PEG crystalline regions. On the PEG-PCL spectra, new absorbances emerge; one at 1724 cm^{-1} is attributed to stretching of the esteric carbonyl, while the two at 2935 and 729 cm^{-1} are due to C-H bond stretching in the PCL block. All absorbancies attributed to the PCL block increase in intensity from PEG-PCL-1 to PEG-PCL-4, as the molecular weight of the hydrophobic block increases respectively.

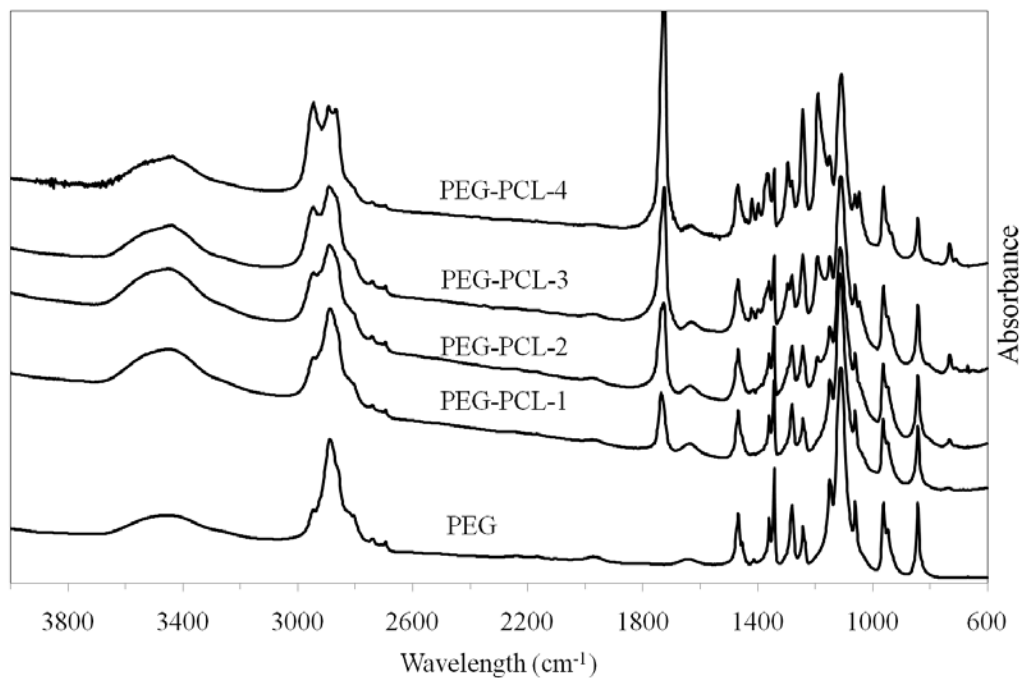


Figure 2. FT-IR spectra for PEG and the synthesized copolymers.

Nuclear magnetic resonance spectroscopy (NMR). Chemical structure, proton numbering and ¹H-NMR spectra for polymers is shown in Figure 3.

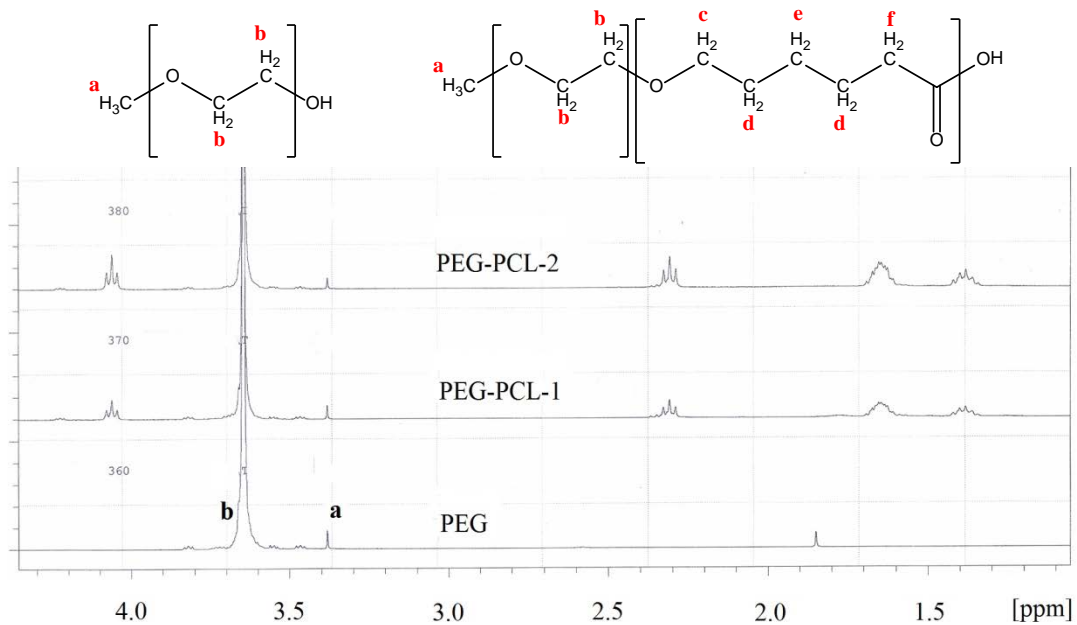


Figure 3. Proton numbering and $^1\text{H-NMR}$ spectra for PEG and synthesized di-block PEG-PCL copolymers.

The degree of polymerization, DP, of PCL was calculated using the equation:

$$\text{DP}_{\text{PCL}} = (A_{4.0}/2)/(A_{3.3}/3) = (A_{2.3}/2)/(A_{3.3}/3) \quad (3)$$

Absorbancies at 4.0 and 2.3 δ are due to protons in the PCL block, while the absorbance at 3.3 δ is due to the three protons in the methoxy terminal-group of PEG. This allowed the calculation of the molecular weight for each polymer using NMR spectroscopy. The M_n results presented in Table 2 are in relatively good agreement with those obtained using GPC.

Table 2. Degree of polymerization, DP, and number average molecular weight, M_n , of the synthesized copolymers, as determined by $^1\text{H-NMR}$.

Polymer	DP	M_n (Da)
PEG-PCL-1	10	7300
PEG-PCL-2	13	7600
PEG-PCL-3	31	9600
PEG-PCL-4	54	12300

Parameters Affecting the Micellization Process. Membrane Used. In order to investigate the role of membrane during micellization process, two micelle suspensions were prepared under the same operating conditions (agitation speed = 700 rpm and organic phase flow rate = 4 ml min $^{-1}$) and using the same formulation (polymer PEG-PCL-4 concentration = 1 mg ml $^{-1}$, organic solvent = THF, and aqueous to organic phase volume ratio = 5). In one experiment, the organic phase was injected directly in the aqueous phase, whereas in another experiment

the organic phase was passed through the membrane with a pore size of 20 μm and pore spacing 80 μm . As shown in Figure 4, the mean particle size of micelle suspension was 552 nm for direct injection and 132 nm for injection through the membrane. In direct injection micromixing occurs after macromixing (breaking macrovolumes of the organic phase into microvolumes by agitation), whereas in membrane injection micromixing is a sole means of mixing. Therefore, membrane injection is associated with better uniformity of polymer and organic solvent distribution through the aqueous phase resulting in a more uniform distribution of micelle sizes and significantly smaller particle size.

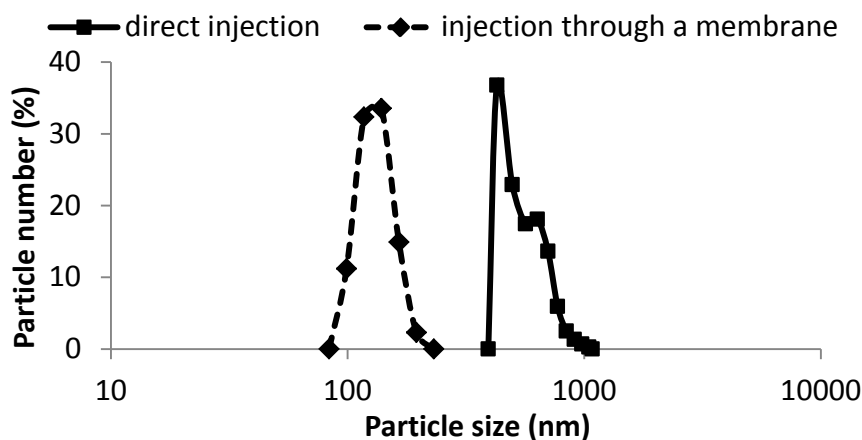


Figure 4. Size distribution of micelles prepared by direct or membrane injection of the organic phase. Experimental conditions: organic phase flow rate = 4 ml min⁻¹, membrane pore size = 20 μm , pore spacing = 80 μm , polymer PEG-PCL-4 concentration = 1 mg ml⁻¹, organic solvent = THF, agitation speed = 700 rpm, aqueous to organic phase volume ratio = 5.

Aqueous to Organic Phase Volume Ratio, AOR. The particle size distribution of micelles was compared by injecting 5 ml of the organic phase through the membrane into respectively 15, 25 and 35 ml of water (corresponding to an AOR of 3, 5 and 7). As shown in Table 3 and Figure 5(a), when the AOR increased from 3 to 7, the mean micelle size decreased from 127 to 90 nm and the PDI increased from 0.24 to 0.29. A similar behavior was observed during

fabrication of liposomes in a hollow fiber module, with the particle size reduction from 189 to 114 nm as a result of increase in AOR from 0.4 to 2.³⁰ By increasing AOR, the polymer is more rapidly dispersed in the aqueous phase due to a higher concentration gradient during mixing and the critical micellar concentration (CMC) is reached faster, which means that less time is allowed for the polymer molecules to redistribute into larger micelles. In addition, at the higher AOR value, micelles are more diluted after mixing with the aqueous phase, which may reduce their tendency to aggregation. Based on the obtained results and taking into consideration the final micelle concentration and their size and uniformity, the AOR was fixed at 5 in the following experiments.

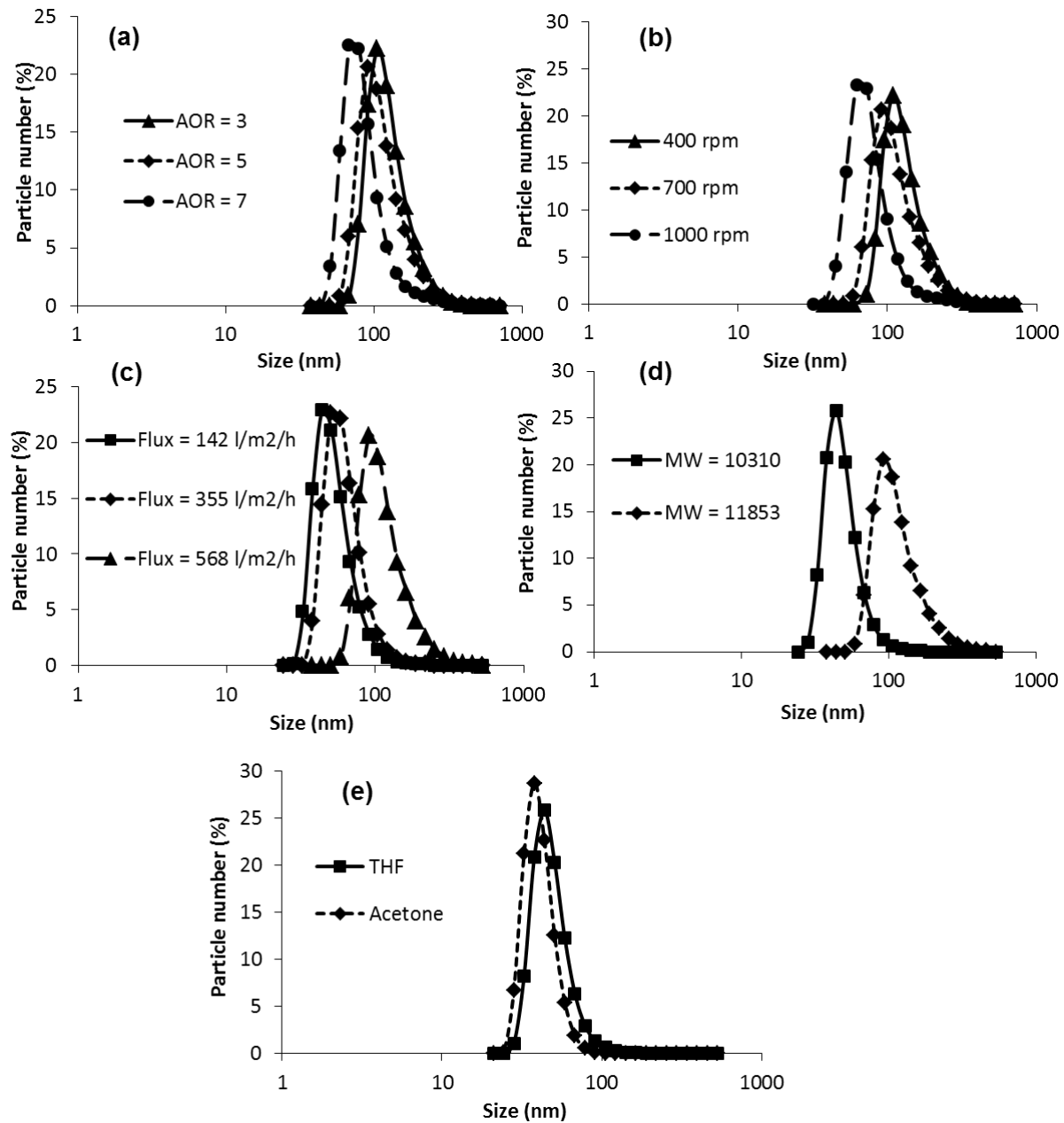


Figure 5. The effect of different process parameters on the micelle size distribution: (a) Aqueous to organic phase volume ratio, AOR, (b) Agitation speed, (c) Transmembrane flux, (d) Polymer molecular weight, and (e) Type of the organic solvent. Other conditions are specified in Table 3.

Table 3. Influence of formulation factors and process parameters on micelle size characteristics. The membrane pore size was 20 μm and the interpore distance was 200 μm .

AOR	Agitation speed (rpm)	Flux ($l\ m^{-2}\ h^{-1}$)	Polymer used	Organic solvent	Mean size (nm)	PDI	Zeta potential (mV)
3	700	568	PEG-PCL-4	THF	127	0.24	-20.1
5	700	568	PEG-PCL-4	THF	117	0.28	-27.6
7	700	568	PEG-PCL-4	THF	90	0.29	-24.2
5	400	568	PEG-PCL-4	THF	131	0.24	-24.8
5	1000	568	PEG-PCL-4	THF	82	0.41	-24.0
5	700	142	PEG-PCL-4	THF	54	0.23	-26.1
5	700	355	PEG-PCL-4	THF	62	0.26	-24.2
5	700	568	PEG-PCL-3	THF	49	0.36	-26.8
5	700	568	PEG-PCL-3	Acetone	41	0.47	-25.0

Agitation Speed. The influence of agitation speed over a range of 400-1000 rpm on the micelle size is shown in Table 3 and Figure 5(b). The micelle size decreased from 131 to 82 nm when the agitation speed increased from 400 to 1000 rpm and the most uniform micelles (PDI = 0.24) were obtained at the stirring rate of 400 rpm. The shear stress at the membrane/continuous phase interface increases with increasing the stirring rate. It was previously found that the particle size in membrane-based particle fabrication processes was smaller at the higher wall shear stress,^{24,31} which was associated with higher mixing efficiency.^{32,33} Thus, high homogenous supersaturation may occur in a short time, leading to rapid self-arrangement of polymers and formation of small micelles. Our results suggest that for a given set of conditions, an agitator speed of 700 rpm was the optimal speed, since the produced micelles were both relatively uniform and of suitable size.

Transmembrane Flux. As shown in Table 3 and Figure 5(c), by increasing the dispersed phase flux from 142 to 568 $l\ m^{-2}\ h^{-1}$, the mean micelle size increased from 54 to 117 nm and

PDI increased from 0.23 to 0.28. The higher dispersed phase flux resulted in the higher amount of the polymer injected through the membrane per unit time,³⁴ which has an effect to prolong mixing time and reduce the mixing efficiency. The maximum micelle size in Table 3 corresponds to the maximum polymer concentration at the membrane/continuous phase interface. Thus, the largest micelles were formed at the maximum transmembrane flux and the minimum agitation speed.

Copolymer Molecular Weight, MW. The results in Table 3 and Figure 5(d), show that larger micelles were prepared using a copolymer with the higher MW. Both polymers are suitable for preparation of micelles with a convenient mean size (between 49 and 117 nm) and acceptable size distribution (PDI between 0.26 and 0.36) for drug release applications.

Organic Solvent. Numerous organic solvents have been used for micelle preparation, such as methanol,³⁵ THF,³⁶ dimethylsulfoxide,³⁷ N,N-dimethylformamide, and acetone.³⁸ Although removed by evaporation, solvents may remain as traces in the final formulation, representing a possible risk for human health. In this work, THF and acetone were selected as organic solvents due to their low toxicity and good vitamin E and PEG-PCL solubility. Table 3 and Figure 5(e) show that the particle size distribution is virtually unaffected by the organic solvent used.

Membrane structure. Micelle suspensions were prepared using 6 different membranes with pore diameters of 5, 10, 20 and 40 μm and pore spacing of 80 or 200 μm . At the constant pore spacing of 200 μm , a strong linear correlation between the mean micelle size and the membrane pore size was found, with a gradient of 2 nm μm^{-1} and $R^2 > 0.99$, as shown in Figure 6. A similar linear relation between the particle size and pore size of microengineered

membrane was obtained in fabrication of liposomes³⁹ and membrane emulsification.⁴⁰⁻⁴¹ The results clearly show that the micelle size can be controlled by the membrane pore size. The size uniformity increased with decreasing the pore size (Figure 6b). As shown in Table 4, the micelle size decreased by 4-10 % as a result of increase in the pore spacing from 80 to 200 μm . There are two consequences of increasing pore spacing at constant transmembrane flux: (i) organic phase stream is fragmented into smaller number of sub-streams, and (ii) the flow velocity of each sub-stream is higher. The micromixing is more efficient when at the higher velocity of organic phase, probably because the organic phase micro-jets can penetrate deeper into the aqueous phase before being disintegrating due to mixing with a surrounding aqueous phase.

Table 4. Influence of membrane on the micelle size characteristics. The experimental conditions: aqueous to organic phase volume ratio AOR = 5, organic solvent = THF, polymer PEG-PCL-4 concentration: 1 mg ml^{-1} , agitation speed = 700 rpm, transmembrane flux = $568 \text{ l m}^{-2} \text{ h}^{-1}$.

Membrane characteristics		Micelles size characteristics	
Spacing (μm)	Pore size (μm)	Mean size (nm)	PDI
200	5	92	0.17
	10	101	0.19
	20	117	0.28
	40	165	0.38
80	10	105	0.21
	20	130	0.23

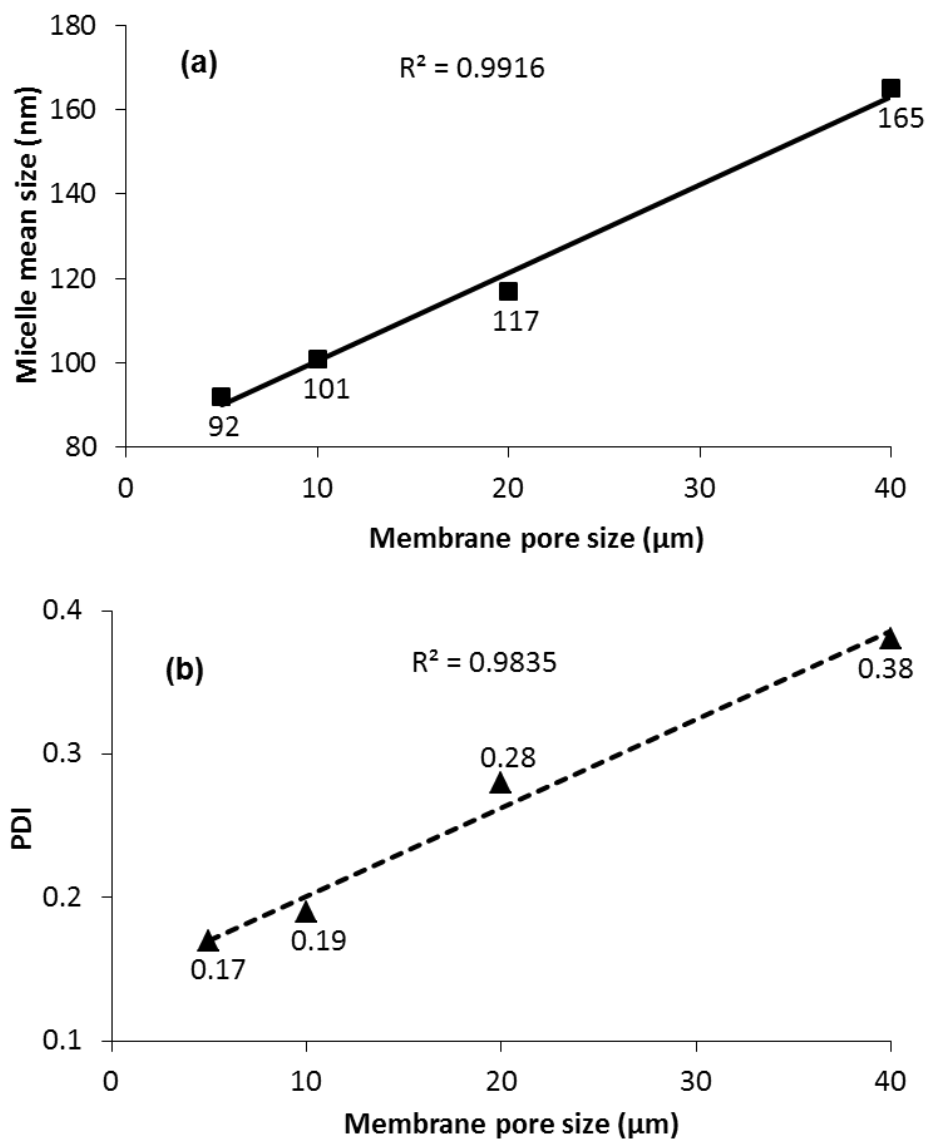


Figure 6. Effect of the membrane pore size on the micelle size characteristics: (a) mean micelle size, and (b) PDI of the micelles. The membrane pore spacing is 200 μm and other conditions are specified in Table 4.

Vitamin E Loading. Vitamin E was chosen as a hydrophobic drug for the preparation of drug-loaded micelles. This active agent was widely used as an antioxidant in many medical and cosmetic preparations and was encapsulated in the micelles by hydrophobic forces, due to its affinity to the hydrophobic block of the copolymers, without chemical conjugation. The effect of drug entrapment on the vesicle size and zeta potential is presented in Table 5 and

Figure 7. The mean micelle size increased from $d_0 = 92$ to $d_1 = 154$ nm when vitamin E was encapsulated under otherwise constant experimental conditions. Thermodynamically stable drug-loaded micelles can be referred to as “microemulsion droplets” or “swollen micelles” and these two terms can be used interchangeably.⁴² Although there is no single particle size that can be used as a definitive cut-off point to distinguish a swollen micelle from a conventional emulsion, most authors assume that the mean particle diameter in a stable O/W microemulsion should be less than 200 nm.⁴³ Assuming that the micelles are spherical and volumes of vitamin E and copolymer are additive, the drug loading percentage is as follows:

$$\text{Loading}(\%) = \frac{\text{Mass of drug in a micelle}}{\text{Mass of drug-loaded micelle}} \times 100 = \frac{(d_1^3 - d_0^3)\rho_E}{(d_1^3 - d_0^3)\rho_E + d_0^3\rho_{\text{PEG-PCL}}} \times 100 \quad (3)$$

where $\rho_E = 0.95 \text{ g ml}^{-1}$ is the density of vitamin E and $\rho_{\text{PEG-PCL}} = 1.135 \text{ g ml}^{-1}$ is the density of PEG-PCL diblock copolymer, based on melt densities of PEG and PCL homopolymers of 1.13 and 1.4 g ml^{-1} , respectively. The drug loading calculated using Eq. (3) is 75%, which means that vitamin E constitutes 75% of the total mass of a drug-loaded micelle and the copolymer 25%. The drug loading can be also estimated from the mass balance of vitamin E. It is reasonable to suggest that neither vitamin E nor copolymer was adsorbed onto the membrane surface due to low internal pore volume of the membrane. The volume of organic phase injected through the membrane was 5 ml, the concentration of vitamin E in the organic phase was 2.5 mg ml^{-1} and the efficiency of vitamin E encapsulation was 87.4 % (Table 5), which means that the total amount of vitamin E entrapped within the micelles was 10.9 mg. The critical micelle concentration (CMC) of PEG-PCL diblock copolymer with a molecular weight of 12600 Da, as determined by GPC, was found to be 0.018 mg ml^{-1} .⁴⁴ The total amount of non-aggregated PEG-PCL-4 molecules in the final preparation was 0.45 mg, based

on the volume of aqueous phase in the final preparation of 25 ml and the above value of CMC. The concentration of PEG-PCL-4 in the organic phase was 1.0 mg ml^{-1} and thus, the total amount of PEG-PCL-4 incorporated in the micelles was 4.55 mg. The drug loading estimated from the process mass balance is now: $10.9/(4.55+10.9) \times 100 = 71\%$, which is close to 75%, calculated from Eq. 3. A small difference can be attributed to the fact that Eq. (3) does not take into account the effect of molecular interactions on the volumes of vitamin E and copolymers in the micelles.

The zeta-potential of vitamin E-loaded micelles and drug-free micelles was -19.3 and -27.0 mV, respectively (Table 5), which can be attributed to the presence of terminal carboxyl groups on PCL chains. Zeta potential measurements can give information about the type of association between the active substance and the carrier,⁴⁵ for example whether the drug is encapsulated in the core material or adsorbed onto the shell.⁴⁶ Here, the negative surface charge was partially shielded in the presence of the drug suggesting that at a small part of the drug might have been adsorbed onto the surface, while the rest was incorporated within the micelle cores. The zeta potential data suggest that the micelles should exhibit a good colloidal stability, since a negative zeta potential near or lower than -20 mV was found to prevent vesicle coalescence.⁴⁷ A high encapsulation efficiency of 87.4% was probably due to the high hydrophobicity of the vitamin E as many studies reported that the encapsulation efficiency was proportional to the drug solubility in the organic phase.⁴⁸ Drug-loaded micelles were more uniform in size than unloaded micelles as evidenced by the lower PDI value in Table 5. It was found that core-entrapping drug, in this case α -tocopherol, may act as a filler molecule and enhance the stability of the micelle.⁴⁹

Table 5. The effect of vitamin E loading on the micellization process. Organic solvent: THF, polymer PEG-PCL-4 concentration = 1 mg ml⁻¹, vitamin E concentration in the organic phase = 2.5 mg ml⁻¹, agitation speed = 700 rpm, AOR = 5, transmembrane flux = 568 l m⁻² h⁻¹.

	Size (nm)	PDI	Zeta potential (mV)	Encapsulation efficiency (%)
Drug-free micelles	92	0.17	-27.0	
Drug-loaded micelles	154	0.09	-19.3	87.4

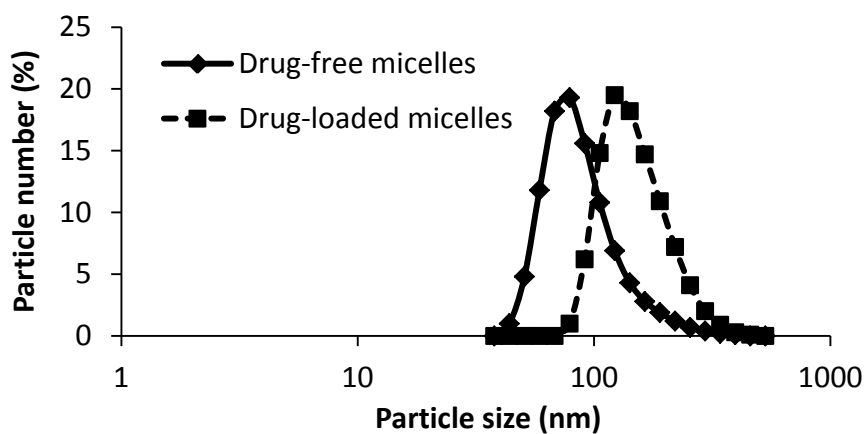


Figure 7. The effect of loading vitamin E into micelles on their size distribution. The experimental conditions are specified in Table 5.

Process Reproducibility. The reproducibility of the preparation technique was investigated by repeating 3 times a typical micellization experiment with and without drug loading. The results in Figure 8 and Table S2 suggest a very good reproducibility in terms of size characteristics, zeta potential and encapsulation efficiency between the samples produced under the same conditions.

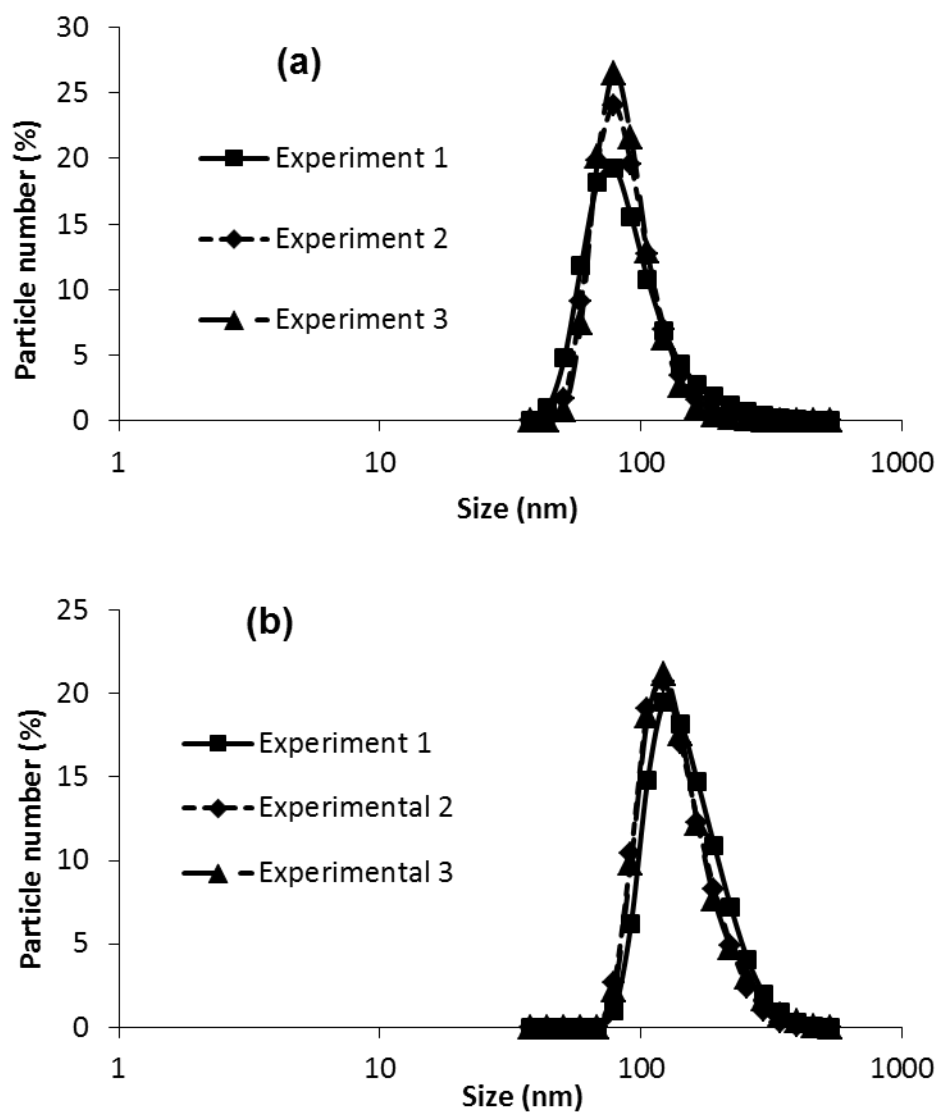


Figure 8. Reproducibility of the micelle preparations: (a) Drug-free micelles and (b) Drug-loaded micelles. Experimental conditions are specified in Table 5.

TEM Observation. Figure 9 revealed nanometric, quasi-spherical shape of vitamin E-loaded micelles. According to this morphological investigation, micelles ranged in size from 100 to 200 nm, which is in good correlation with the dynamic light scattering measurements.

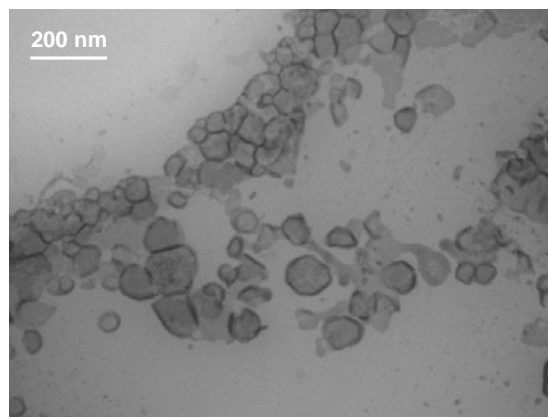


Figure 9. TEM micrograph of vitamin E-loaded micelles.

pH-Responsive Drug Release. The release of vitamin E from micelle preparations stored under different pH conditions was monitored as a function of time. The results in Figure 10 show that the micelles kept under acidic pH were unstable due to hydrolysis of the ester bonds in the PCL block and formation of 6-hydroxycaproic acid. Since vitamin E is predominantly encapsulated within a hydrophobic core, hydrolytic degradation of hydrophobic PCL segments led to the release of vitamin E. A decrease in the drug encapsulation efficiency was proportional to the medium acidity, because PCL hydrolysis was catalyzed by hydrogen ions. Indeed, within 50 hours, the encapsulation efficiency decreased from an initial value of 89.2% to 83.2, 79.5 and 68.3% at the pH of 6.3, 4.5 and 1.9, respectively. When the micelles were stored at the pH of 9.8, no release of vitamin E occurred and the encapsulation efficiency remained nearly unchanged.

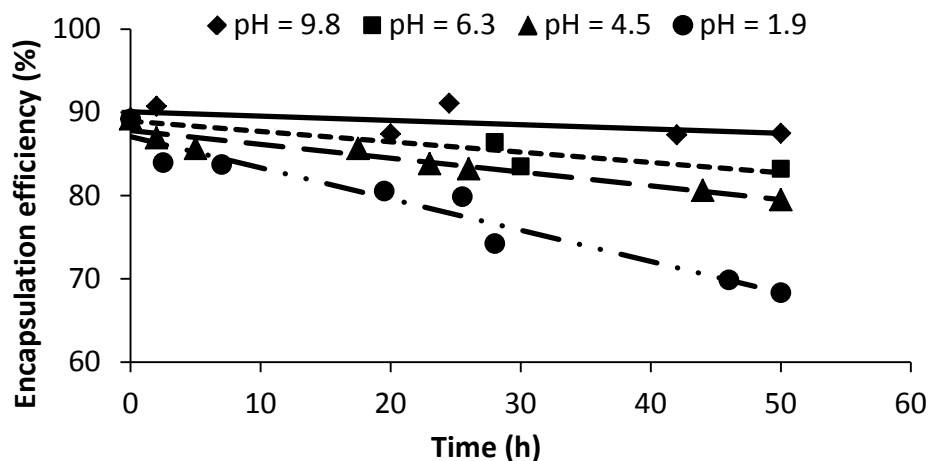


Figure 10. Time evolution of the encapsulation efficiency of vitamin E-loaded micelles stored under different pH conditions.

Preparation of PEG-Hyd-PCL Micelles. The maximum percent of vitamin E released from PEG-PCL micelles after 50 h was 23 % at pH = 1.9. In order to increase the release rate and pH sensitivity at mildly acidic pH, we have synthesized highly pH sensitive PEG-Hyd-PCL micelles by incorporating a pH-sensitive hydrazone bond between the PEG and PCL blocks. When the micelles are exposed to mildly acidic pH, the bond hydrolyzes and the micelle collapses releasing the drug. We have prepared PEG-PCL and PEG-Hyd-PCL micelles under the same conditions by transferring 5 ml of the organic phase containing 5 mg ml⁻¹ of each polymer dissolved in THF to 25 ml of deionized water at the flow rate of 0.5 ml min⁻¹ and pH = 7.4 to obtain the final micelle concentration of 1 mg ml⁻¹ and AOR = 5. The micelle suspension was gently stirred for 6 hours and any residual THF was removed with vacuum distillation. As can be seen in Figure 11, both micelle types were found to show identical micellization behaviour forming micelles of identical particle size distribution. It shows that the micellization behavior is determined only by the type of the hydrophobic and hydrophilic block and molecular weight of the polymer and not by the presence of hydrazone bond. The

main difference between the two micelle types was in a higher pH sensitivity of PEG-Hyd-PCL micelles. We have confirmed the hydrolysis of hydrazone bond by GPC, showing bimodal MW distributions in PEG-Hyd-PCL dispersions exposed to $\text{pH} < 6$, whereas the MW distribution was monomodal at neutral pH. The hydrolysis leads to the dissolution of the PEG blocks and the release of the PCL blocks and the entrapped drug. This was confirmed by optical transmittance and DLS measurements in PEG-Hyd-PCL dispersions at $\text{pH} < 6$. By decreasing pH, the transmittance of PEG-Hyd-PCL dispersions at 500 nm decreased significantly, while the average particle size increased, which can be both explained by the agglomeration of released PCL blocks.

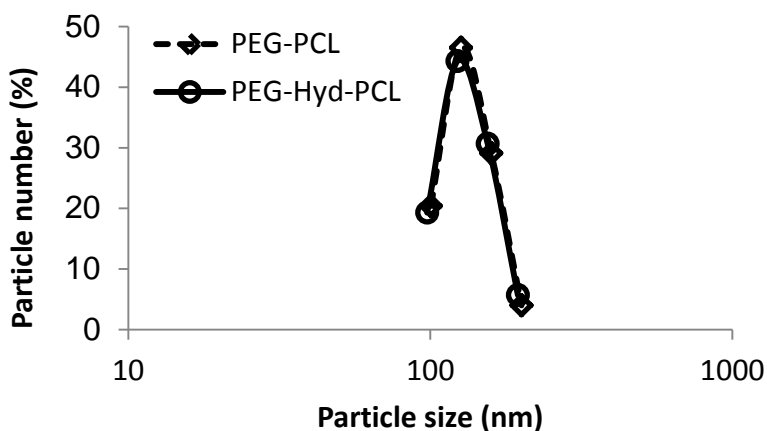


Figure 11. Particle size distributions of micelles composed of PEG-PCL and PEG-Hyd-PCL copolymers. The molecular weight of PEG and PCL block was the same in both copolymers.

CONCLUSIONS

Di-block copolymers composed of hydrophilic poly(ethylene) glycol (PEG) and hydrophobic polycaprolactone (PCL) segments were successfully synthesized, characterized, and used for the preparation of pH sensitive PEG-PCL micelles using a new membrane dispersion method. The organic phase composed of a mixture of the copolymer and a volatile organic solvent was

split into numerous microscopic sub-streams by injection through a microsieve membrane and mixed with an agitated aqueous phase. A precise control over the micelle size and size distribution was achieved by controlling the pore size and interpore distance of the membrane, molecular weight of the copolymer, solvent type, and micromixing conditions in the stirred cell device, such as transmembrane flux, aqueous to organic phase ratio, and agitation speed. The micelles were obtained with a sufficiently small mean size, satisfying zeta potential, and high encapsulation efficiency of a hydrophobic drug (vitamin E), and can be used as a pH-sensitive delivery system. The preparation technique is simple, fast, reproducible, and has a potential for an industrial scale-up.

ASSOCIATED CONTENT

Supporting Information. The supporting information includes the microscopic images of membrane surface, properties of the membrane used and the reproducibility data for the process. This material is available free of charge via the Internet at <http://pubs.acs.org>.

ACKNOWLEDGMENT

Abdallah LAOUINI held a CMIRA Explora fellowship from “Région Rhône-Alpes”. The additional funding came from The Engineering and Physical Sciences Research Council of the United Kingdom (reference number: EP/HO29923/1).

REFERENCES

- (1) Wein, H.; Zhang, X.; Zhou, Y.; Cheng, S.; Zhuo, R. *Biomaterials*. **2006**, *27*, 2028–2034.
- (2) Du, J.; O’Reilly, R. K. *Soft Matter*. **2009**, *5*, 3544–3561.

- (3) Grislain, L.; Couvreur, P.; Lenaerts, V.; Roland, M.; Deprez-Decampeneere, D.; Speiser, P. *Int. J. Pharm.* **1983**, *15*, 335–345.
- (4) Maeda, H. *Adv. Enzyme Regul.* **2001**, *41*, 189–207.
- (5) Ganta, S.; Devalapally, V. P.; Shahiwala, A.; Amiji, M. *J. Controlled Release.* **2008**, *126*, 187–204.
- (6) Engin, K.; Leeper, D. B.; Cater, J. R.; Thistlethwaite, A. J.; Tupchong, L.; MacFarlane, J. D. *Int. J. Hyperthermia.* **1995**, *11*, 211–216.
- (7) Gillies, E. R.; Fréchet, J. M. *J. Chem. Commun.* **2003**, *14*, 1640–1641.
- (8) Chen, W.; Meng, F. H.; Li, F.; Ji, S. J.; Zhong, Z. Y. *Biomacromolecules.* **2009**, *10*, 1727–1735.
- (9) Tang, R.; Ji, W.; Panus, D.; Palumbo, R.N.; Wang, C. *J. Controlled Release.* **2011**, *151*, 18–27.
- (10) Yang, L.; Wu, X.; Liu, F.; Duan, Y.; Li, S. *Pharm. Res.* **2009**, *26*, 2332–2342.
- (11) Liggins, R. T.; Burt, H. M. *Adv. Drug Delivery Rev.* **2002**, *54*, 191–202.
- (12) Zeng, F.; Liu, J.; Allen, C. *Biomacromolecules.* **2004**, *5*, 1810–1817.
- (13) Yokoyama, M.; Opanasopit, P.; Okano, T.; Kawano, K.; Maitani, Y. *J. Drug Targeting.* **2004**, *12*, 373–384.
- (14) Vangeyte, P.; Gautier, S.; Jérôme, R. *Colloids Surf., A.* **2004**, *242*, 203–211.
- (15) Kohori, F.; Yokoyama, M.; Sakai, K.; Okano, T. *J. Controlled Release.* **2002**, *78*, 155–163.
- (16) Aliabadi, H. M.; Elhasi, S.; Mahmud, A.; Gulamhusein, R.; Mahdipoor, P.; Lavasanifar, A. *Int. J. Pharm.* **2007**, *329*, 158–165.

- (17) Elhasi, S.; Astaneh, R.; Lavasanifar, A. *Eur. J. Pharm. Biopharm.* **2007**, *65*, 406–413.
- (18) Tyrrell, Z. L.; Shen, Y.; Rados, M. *Prog. Polym. Sci.* **2010**, *35*, 1128–1143.
- (19) Aliabadi, H. M.; Lavasanifar, A. *Expert Opin Drug Deliv.* **2006**, *3*, 139–162.
- (20) Vladisavljević, G. T.; Williams, R. A. *Adv. Colloid Interface Sci.* **2005**, *113*, 1–20.
- (21) Charcosset, C.; El Harati, A.; Fessi, H. *J. Controlled Release.* **2005**, *108*, 112–120.
- (22) Laouini, A.; Jaafar-Maalej, C.; Sfar-Gandoura, S.; Charcosset, C.; Fessi, H. *Prog. Colloid Polym. Sci.* **2012**, *139*, 23–28.
- (23) Laouini, A.; Fessi, H.; Charcosset, C. *J Membr. Sci.* **2012**, *423–424*, 85–96.
- (24) Vladisavljević, G. T.; Kobayashi, I.; Nakajima, M. *Microfluid. Nanofluid.* **2012**, *13*, 151–178.
- (25) Kölchens, S.; Ramaswamia, V.; Birgenheiera, J. *Chem. Phys. Lipids.* **1993**, *65*, 1–10.
- (26) Provder, T. *Prog. Org. Coat.* **1997**, *32*, 143–153.
- (27) Hunter, R.; Midmore, H. Z. *J. Colloid Interface Sci.* **2001**, *237*, 147–149.
- (28) Laouini, A.; Jaafar-Maalej, C.; Limayem-Blouza, I.; Sfar-Gandoura, S.; Charcosset, C.; Fessi, H. *J. Colloid Sci. Biotechnol.* **2012**, *1*, 147–168.
- (29) Discher, D. E.; Eisenberg, A. *Science.* **2002**, *297*, 967–973.
- (30) Laouini, A.; Jaafar-Maalej, C.; Sfar-Gandoura, S.; Charcosset, C.; Fessi, H. *Int. J. Pharm.* **2011**, *415*, 53–61.
- (31) Kobayashi, I.; Yasuno, M.; Iwamoto, S.; Shono, A.; Satoh, K.; Nakajima, M. *Colloids Surf., A.* **2002**, *207*, 185–196.

- (32) Jaafar-Malej, C.; Diab, R.; Andrieu, V.; Elaissari, A.; Fessi, H. *J. Liposome Res.* **2010**, *20*, 228–23.
- (33) Zhang, Y. L.; Frangos, J. A.; Chachisvilis, M. *Biochem. Biophys. Res. Commun.* **2006**, *347*, 838–841.
- (34) Xu, J. H.; Luo, G. S.; Chen, G. G.; Wang, J. D. *J. Membr. Sci.* **2005**, *266*, 121–131.
- (35) Li, X.; Zhang, Y.; Fan, Y.; Zhou, Y.; Wang, X.; Fan, C.; et al. *Nanoscale Res. Lett.* **2011**, *6*, 275–283.
- (36) Huang, X.; Xiao, Y.; Lang, M. *J. Colloid Interface Sci.* **2011**, *364*, 92–99.
- (37) Yin, H.; Bae, Y. H. *Eur J. Pharm. Biopharm.* **2009**, *71*, 223–230.
- (38) Qiu, L.; Zheng, C.; Jin, Y.; Zhu, K. *Expert Opin. Ther. Pat.* **2007**, *17*, 819–830.
- (39) Laouini, A.; Charcosset, C.; Fessi, H.; Holdich, R. G.; Vladisavljević, G. T. *RSC Adv.* **2013**, *3*, 4985–4994.
- (40) Dragosavac, M. M.; Holdich, R. G.; Vladisavljević, G. T.; Sovilj, M. N. *J. Membr. Sci.* **2012**, *392–393*, 122–129.
- (41) Vladisavljević, G. T.; Schubert, H. *J. Membr. Sci.* **2003**, *225*, 15–23.
- (42) Mitchell, J.; Ninham, B. W. *J. Chem. Soc., Faraday Trans.* **1981**, *77*, 601–629.
- (43) McClements, D. J. *Soft Matter.* **2012**, *8*, 1719–1729.
- (44) Sun, H.; Guo, B.; Cheng, R.; Meng, F.; Liu, H.; Zhong, Z. *Biomaterials.* **2009**, *30*, 6358–6366.
- (45) McClements, D. J. *Food Emulsions*, 2nd Edition, CRC Press; Boca Raton, 2005, pp. 191.
- (46) Brratt, G. *Cell. Mol. Life Sci.* **2003**, *60*, 21–37.
- (47) Wiacek, A.; Chibowski, E. *Colloids Surf., A.* **1999**, *159*, 253–261.

(48) Xu, Q.; Tanaka, Y.; Czernuszka, J. T. *Biomaterials*. **2007**, *28*, 2687–2694.

(49) Kataoka, K.; Harada, A.; Nagasaki, Y. *Adv. Drug Delivery Rev.* **2001**, *47*, 113–131.

Table of Contents Graphic

